Journal of Power Sources 196 (2011) 6822–6827

Contents lists available at ScienceDirect

Journal of Power Sources

journal homepage: www.elsevier.com/locate/jpowsour

Lithium intercalation reaction into the Keggin type polyoxomolybdates

Noriyuki Sonoyama*, Yoshiaki Suganuma, Tomohiro Kume, Zhen Quan

Department of Materials Science and Engineering, Nagoya Institute of Technology, Gokiso-cyo, Showa-ku, Nagoya 466-8555, Japan

ARTICLE INFO

Article history:
Received 12 August 2010
Received in revised form
28 September 2010
Accepted 29 September 2010
Available online 7 October 2010

Keywords:
Lithium intercalation
Cluster ions
Keggin type polyoxometalates

ABSTRACT

The electrochemical property of Keggin type hetero polyoxomolybdate $K_3[PMo_{12}O_{40}]$ (KPM) as the cathode electrode material for lithium battery was examined. KPM showed charge–discharge performance in the potential region from 4.2 V to 1.5 V with capacity of over 200 mAh g^{-1}. From the result of the ex situ XRD measurement, it is presumed that the electrochemical reaction of KPM proceeds via the lithium (de-)intercalation. The cycle performance of KPM is largely dependent on the charge–discharge potential range. The capacity fade caused by deep discharging seems to be concerned to the ⟨ to ® isomerization of KPM.

1. Introduction

Lithium batteries are a promising energy storage source for the next generation electric devices, e.g. hybrid vehicle and pure electric vehicle. At present, the currently using cathode materials for the lithium battery are the intercalation materials of metal oxide or phosphate including lithium ion in their lattices. For these materials the capacity is mainly determined by the re-productivity of the structure during the lithium (de-)intercalation.

Contrary to these lithium (de-)intercalation materials, the cathode materials, so called 'organic radical cell' that lithium intercalation does not proceed in the charge–discharge process, has developed [1–4]. In the discharge process of the organic radical cell, discharge proceeds by electrochemical anion radical formation and concurrent lithium adsorption to the electrode surface. For this type of electrodes, the redox active part for electrochemical reaction is very small and independent from the crystal structure, because redox occurs at the molecules connected with polymer media. The capacity is almost equal to the amount of the redox active part contained in the materials. The organic radical cell shows comparatively faster charge–discharge performance, without slow lithium intercalation in charge–discharge process, than the lithium intercalation materials, though the durability of the organic electrode materials is apprehensive.

The metal complexes were expected to show unique electrochemical properties as the electrode for lithium battery with independent redox center and characteristic crystal structure. Yamaki et al. have reported that metal-phthalocyanines show lithium intercalation activity with high capacity. [5,6] Imanishi et al. also reported the lithium intercalation into the ferrocyanide [7,8]. The structures of these complexes are rather like organic compounds or metal oxide and do not show much different property from the organic compounds and oxide materials, respectively. The cluster ion electrodes are also expected to show the intermediate property between the lithium intercalation electrodes and the organic radical electrodes. Usual cluster ions consist of several or several tens of metal ions in a unit. It behaves as a single molecule under the dissolved condition in solvents. In the solidification process, cluster ions form ionic crystals with some counter ions, while some of them become amorphous. Recently, charge–discharge ability of cluster complex was reported by Yoshikawa et al. [9] using $[Mn_{12}O_{12}(CH_3COO)_{16}(H_2O)_4]$ as a cathode material. This cluster complex shows the initial discharge capacity of over 200 mAh g^{-1}. After the secondary discharge, $[Mn_{12}O_{12}(CH_3COO)_{16}(H_2O)_4]$ showed reversible charge–discharge performance with the capacity around 100 mAh g^{-1}. They also reported that this cluster complex cannot stand under the highly polarized condition because it contains many organic legends (acetic acid ion) for cluster ion formation.

As the candidature for lithium battery cathode material, we focused on Keggin type polyoxomolybdates $K_3PMo_{12}O_{40}$ (KPM). In Fig. 1(a) structure of typical Keggin type hetero polyoxometalates $[(XO_4)(MO_3)_{12}]^{y-}$ (X: Si, P; M: Mo, W, etc.) was shown. Around the tetrahedral agenda ion (X) oxide, MO_6 octahedrons are connected with top or side sharing. From a different point of view, Keggin type polyoxometalates are seen as four $[M_3O_9]$ units are coordinating to the XO_4 ion. In the water or porous organic solvents, $[PM_{12}O_{40}]^{3-}$

* Corresponding author. Tel.: +81 52 735 7243; fax: +81 52 735 7243.
E-mail address: sonoyama@nitech.ac.jp (N. Sonoyama).

0378-7753/$ – see front matter © 2010 Elsevier B.V. All rights reserved.
doi:10.1016/j.jpowsour.2010.09.107

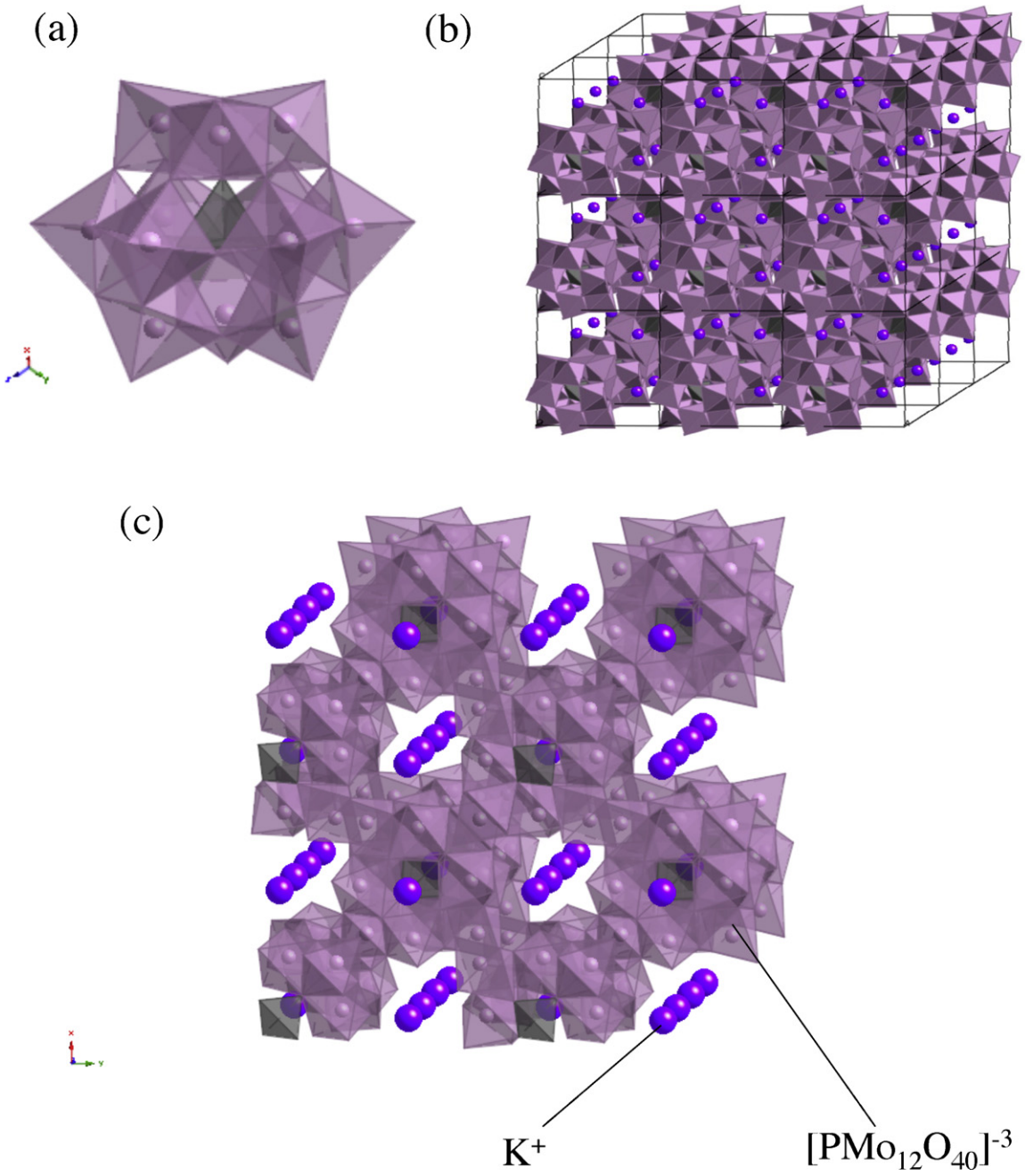

Fig. 1. (a) Structure of Keggin type polyoxometalate (b) and (c) crystal structure of $K_3[PMo_{12}O_{40}]$.

is dissolved and behaves as a single ion. This cluster ion has many open windows and spaces in the cluster ion unit. The widest bottle neck of the window is about 2 Å and this structure may allow the intercalation of the lithium ion whose radius is below 1 Å into the cluster ion itself in principle.

By adding larger cation, e.g. potassium ion, to the solution containing $[PMo_{12}O_{40}]^{3-}$, $K_3PMo_{12}O_{40}$ (KPM) crystal can be obtained. The crystal structure of KPM is shown in Fig. 1(b) and (c) [10]. In the KPM crystal, $[PMo_{12}O_{40}]^{3-}$ ion presents as a separate ion without sharing any atoms with other ions. In principle, $[PMo_{12}O_{40}]^{3-}$ ion and potassium ion locate alternately. KPM crystal has certain amount of vacancies of $[PMo_{12}O_{40}]^{3-}$ ion and K^+ ion occupies this site for charge balance. (Fig. 1(c)) The KPM crystal also has many spaces and tunnels along [1 0 0] and [0 1 1] directions with the radius width of 2.0–2.2 Å. This interstitial space and tunnels will make three dimensional lithium diffusion in the KPM crystal possible, if lithium ion can be intercalated into the KPM. In this crystal structure, redox active unit ($[PMo_{12}O_{40}]^{3-}$) is embedded in the frame work where lithium ion can diffuse along the three dimensional path. Therefore, this material would have both characteristics of lithium intercalation materials and organic electrode material. The former is the frame work that allows the lithium diffusion in crystal and the latter is the scattered "independent" redox active unit to the crystal structure.

In this paper, electrochemical property of KPM was examined as a lithium battery cathode material and its charge–discharge mechanism is studied. With the aim of developing a high capacity cathode material, mechanism of capacity fading was discussed and the improvement of cycle performance was attended.

2. Experimental

Synthesis of $K_3[PMo_{12}O_{40}]$ was carried out via a usual method [11–13]. Identification of products was carried out by XRD measurement using a powder X-ray diffract meter (Rigaku RAD-C) with Cu Kα radiation. Obtained samples were dried at 120 °C for 12 h under air. Annealing treatment was carried out at 200, 300, 400, 500 and 600 °C for 12 h under air. The electrochemical performance of cells was studied by charge–discharge cycle tests and CV measurements using CR-2032 coin cells at 25 °C. The cathode electrode consists of 30 wt% active material, 65 wt% acetylene black and 5 wt% PTFE binder. The electrolyte was ethylene carbonate–diethyl carbonate mixed solvent (1:1) as a solvent with a supporting electrolyte of 1 M $LiPF_6$. The charge–discharge characteristics of the samples were examined using a coin cell with lithium metal as an anode using TOSCAT-5300 battery tester (Toyo System). Cyclic voltamnmetry was measured under the potential control by a potentio-galvanostat (Hokuto HA-501) and a function generator (Hokuto HB-105). AC-impedance spectra for cells were obtained using a frequency-response analyzer (Solatron 1255) connected with the potentiostat (Solatron 1260) in the frequency range 10^{-2} to 10^6 Hz with an applied potential of 0.2 V from the imposed potential. After the charge–discharge measurements, XRD measurement was carried out under Ar atmosphere. ESR measurement was carried out with JEOL RE-1X at room temperature in the magnetic field range of 220–430 mT.

3. Results and discussion

In Fig. 2(a), the XRD pattern for KPM synthesized in this study was shown. All the peaks are agreed with those of KPM in ICSD No. #150445.

In Fig. 3, cyclic voltamograph (CV) for KPM with scan rate 1 mV s^{-1} was shown. Very broad peaks were observed at 3.2, 2.9 and 2.5 V in the anodic scan. The peak separation for the peaks at 3.2 and 2.9 V is very large (about 0.2 V). Only the raise in cathodic current was observed around 2.0 V instead of the apparent peak of cathodic current that corresponds to the anodic current peak at 2.5 V. CV curves of $[PMo_{12}O_{40}]^{3-}$ ion in aqueous-organic mixed solvents and organic solvents were reported by several groups. [14–17] According to these reports, dissolved $[PMo_{12}O_{40}]^{3-}$ shows five or six peaks for two electron redox reaction at the region from −0.8 to +0.3 V vs. SCE. This potential range corresponds to 2.48–3.58 V vs. Li. The profile of CV curve in the present study is much different. The reason for these differences of the CV curve shape between the dissolved ion and solid polycrystalline is not clear. Kulesza et al. measured CV curves for single crystal $H_4SiW_{12}O_{40}{\cdot}31H_2O$, with Keggin structure and reported that single crystal $H_4SiW_{12}O_{40}{\cdot}31H_2O$ showed similar CV curves to the dissolved one in the aqueous solvent. [18] Generally, the CV curves of the solid state compounds are much different from that of the dissolved ion state. This difference would be related to the ion diffusion speed in the crystals. It is known that some of Keggin type hetero polyoxometalates show very high proton conductivity [19], ~0.1 S cm^{-1} at room temperature. For this high proton conductivity comparable to the conductivity of liquid electrolytes, the rate determining step would be the electron transfer at the electrode surface, which is expected to be the rate determining step for dissolved Keggin type hetero polyoxometalates. This similarity in the reaction dynamics seems to be the reason that single crystal $H_4SiW_{12}O_{40}{\cdot}31H_2O$ showed similar CV curves to that of dissolved one. According to the discussion mentioned above, different CV curve shape of KPM between the solid state and dissolved state suggests that the rate-determining step is different between the solid KPM and dissolved $[PMo_{12}O_{40}]^{3-}$ ion for electrochemical reaction. For the redox of solid KPM, lithium ion diffusion step seems to concerning to the rate-determining step.

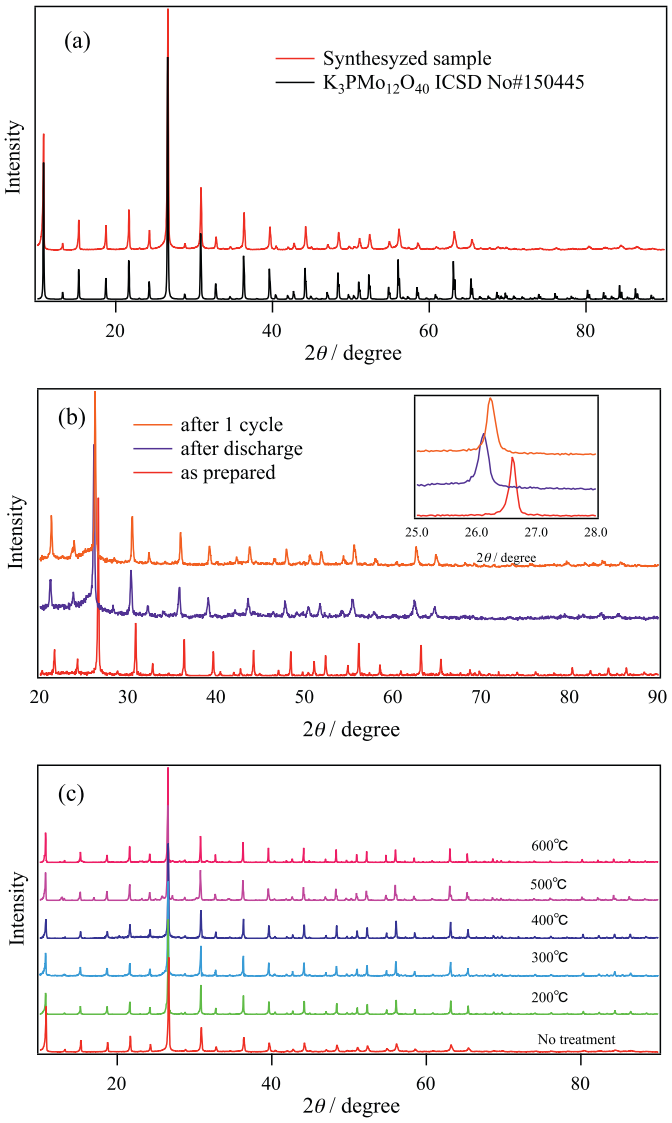

Fig. 2. (a) XRD pattern for $K_3[PMo_{12}O_{40}]$ synthesized in the present study. (b) XRD patterns for $K_3[PMo_{12}O_{40}]$ as synthesized, discharged until 2.0 V and after one cycle discharge–charge. Inset is the close up of the main peak. (c) XRD patterns for $K_3[PMo_{12}O_{40}]$ after annealing at various temperatures.

In Fig. 4(a), the charge–discharge curves for KPM in the voltage range from 3.6 to 2.0 V were shown. In the discharge process, potential decreased linearly and several plateaus appeared at 3.2, 2.9, 2.5 and 2.0 V. This voltage for the plateaus is well agreed with the current peak position of the CV curves (Fig. 3). In the charging process, plateaus were observed at almost the same voltages to those in the discharge process. Open circuit cell voltage showed about 3.3 V at 1 h rest time after charging and the reversible charge–discharge performance was kept after 30 cycles (discussed later). This result evidently indicates that KPM shows reversible charge–discharge ability as a lithium battery cathode.

The electrochemistry of highly reduced Keggin type polyoxometalates has hardly been studied, because Keggin type polyoxometalates dissolved in the organic solvent is not stable under the highly cathodic polarization. On the other hand, many groups have reported some of molybdenum oxides show high capacity as the lithium intercalation materials [20–22]. This high capacity of molybdenum oxides is assignable to the multi step reduction of molybdenum (from +6 to +4). Also for KPM electrode, lithium intercalation in the wide range voltage would be possible as

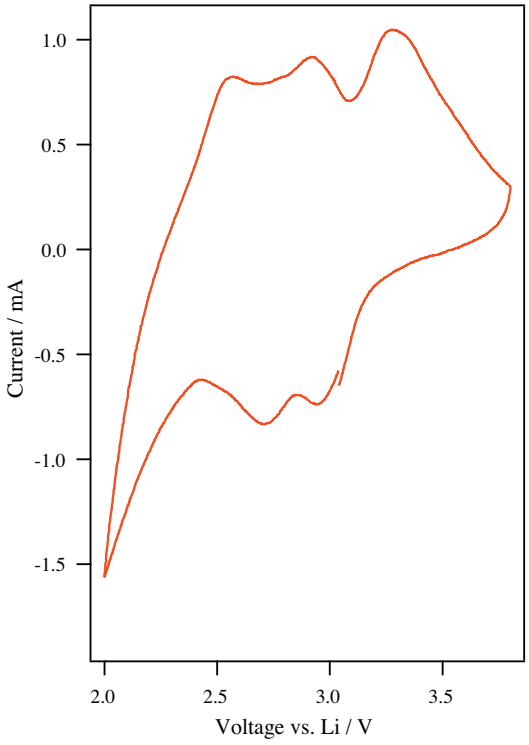

Fig. 3. Cyclic Voltammogram for $K_3[PMo_{12}O_{40}]$ in EC-DEC 1 M $LiPF_6$ vs. Li metal anode.

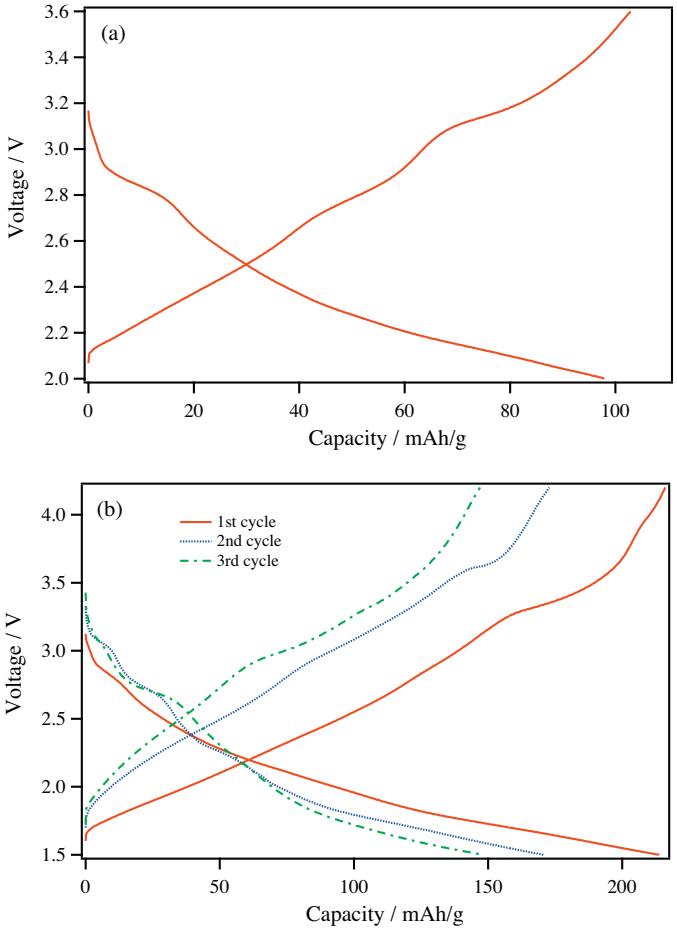

Fig. 4. Charge–discharge curves in the voltage range (a) 3.6–2.0 V (b) 4.2–1.5 V with 50 μA.

long as the structure of KPM is maintained, because KPM crystal has many space to store lithium ion. Fig. 4(b) is the charge–discharge curves for KPM in the voltage range from 4.2 to 1.5 V. Reversible charge–discharge curves for KPM were obtained with the initial capacity of over 200 mAh g^{-1}. This result suggests that multistep reduction of molybdenum proceeds in discharge process of KPM, because the ideal capacity for KPM with single step molybdenum reduction is about 170 mAh g^{-1}. In charging process, in order to obtain the capacity which corresponds with that in discharging process, voltage range was needed to be set to 4.2 V, though the discharge starts at ~3.5 V. This seems to concern with the high electrode resistance of KPM. By AC-impedance measurement, the total electrode resistance at 3.3 V was estimated to be about 1 kΩ.

The energy density of KPM is calculated to be about 480 mWh g^{-1}, which is almost the same value with the current materials (about 500 mWh g^{-1} for $LiCoO_2$, about 400 mWh g^{-1} for $LiMn_2O_4$). This result is due to the lower discharging voltage of KPM, in spite of its high capacity.

To confirm charge–discharge reaction mechanism for KPM, ex situ XRD measurements of KPM after discharge (to 2.0 V) and one cycle discharge–charge process (2.0–4.2 V) were carried out. In Fig. 2(b), XRD patterns for (1) before discharge (as synthesized), (2) after discharge and (3) one cycle discharge–charge process were shown. The inset of Fig. 2(b) is the closed up of the main reflection of KPM in each condition. All the reflections of XRD shifted to lower angle after discharge and then shifted back toward higher angle again by charging without changing the XRD pattern. This result demonstrates that the lattice of KPM crystal expands by lithium intercalation and shrinks reversibly by lithium deintercalation without changing its crystal structure. This result does not agree with the report of Jeannin et al. [23] They obtained single crystal of electrochemically reduced six electron reduced Keggin type polyoxotungstates $Rb_4H_2[H_2W_{12}O_{40}]$ and reported that three tungsten atoms are displaced by 0.48 Å in the direction of the center of a W_3O_9 group. The reason X-ray reflections do not return to the original position is not clear, but isomerization of $[PMo_{12}O_{40}]^{3-}$ ion, mentioned below, may concern with this.

For using KPM as the cathode material of lithium battery, the stability of the reduced KPM crystal should be considered. It is known that deep reduction of $[PMo_{12}O_{40}]^{3-}$ dissolved in the solvent causes α to β isomerization of $[PMo_{12}O_{40}]^{3-}$ ion [24]: one of the $[Mo_3O_9]$ in $[PMo_{12}O_{40}]^{3-}$ rotates 60°. It is also reported that reduced $[PMo_{12}O_{40}]^{(3+y)-}$ is easily hydrolyzed in the aqueous solution. On the other hand, as the solid state oxidizing catalyst, Keggin type polyoxometalates are reported to be very stable even around 400 °C [25] and show very high activity as oxidation- and acid-catalysts [26–28]. In the study about Keggin type polyoxometalates as an oxidizing catalysis including $Cs_3[PMo_{12}O_{40}]$, the mechanism is proposed that the catalytic activity is induced by electron and proton (stored in polyoxometalates) transfer with redox of consistent metal ions of the polyoxometalates [29]. This suggests the solid state polyoxometalates are stable during the repeated redox reaction. The results in the present study also demonstrate that lithium ion reversely intercalates into the crystal of KPM accompanying with the redox of KPM and the crystal structure of KPM is maintained during lithium (de-)intercalation for one cycle discharge–charge process. Though the reason for higher stability for the solid state KPM than the dissolved condition is not clear, it may be explained by the environment around $[PMo_{12}O_{40}]^{3-}$ ion.

For the α to β isomerization of Keggin type polyoxometalates, one of $[Mo_3O_9]$ has to rotate 60°. In the case of the dissolved $[PMo_{12}O_{40}]^{3-}$ anion, there is sufficient cavity for $[Mo_3O_9]$ ion rotation. In addition, the intermediate product of isomerization may be stabilized by the coordination of solvent molecules. On the other hand, in the rigid crystal, the cavity for $[Mo_3O_9]$ rotation is very

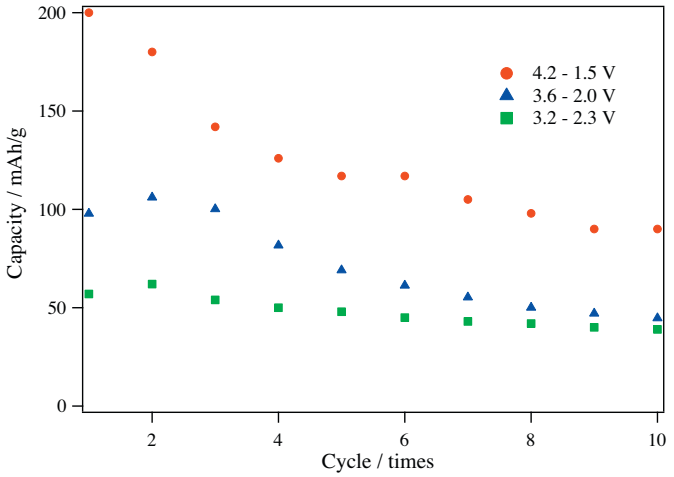

Fig. 5. Relationship between charge–discharge cycles and discharge capacity of $K_3[PMo_{12}O_{40}]$ at various charge–discharge voltage range.

limited. These environmental differences surrounding KPM may suppress the α to β isomerization to a certain extent.

In Fig. 5, cycle dependence of the capacity in the various charge–discharge voltage ranges was shown. The capacity fading rate largely depended on the voltage range. In the voltage region 3.2–2.3 V, discharge capacity hardly changed during 10 cycles, whereas capacity fading speed increased with the increase in the charge–discharge voltage range. Though the detailed mechanism of this capacity fading is not known, this capacity fading seems to be caused by α to β isomerization of a part of $[PMo_{12}O_{40}]^{-3}$ ion. Himeno et al reported that β $[PMo_{12}O_{40}]^{-3}$ ion shows a CV peak at different potential from α type $[PMo_{12}O_{40}]^{-3}$ ion. [23] A new shoulder, appeared in the discharge curve in second and third cycles around 2.6 V in Fig. 4(b), corresponds to reduction of β $[PMo_{12}O_{40}]^{-3}$ ion [23]. This result suggests α to β isomerization is slowly proceeding by deep charge–discharge.

For the improvement of the cycle stability, annealing treatment of KPM was carried out. In Fig. 2(c), the XRD patterns of KPM annealed at 200–600 °C were shown. XRD patterns of KPM annealed at 200–400 °C were hardly changed by annealing treatment. For the sample annealed at 500 °C, new reflections appeared and all of these reflections disappeared by 600 °C annealing. In Fig. 6, the cycle dependence of the capacity of KPM annealed at various temperature with the charge–discharge condition with 50 μA in voltage ranges of 3.6–2.0 V. The cycle stability of KPM is largely dependent on the annealing temperature. The sample annealed at 500 °C showed highest stability and the capacity maintaining ratio was 63% after 30 cycles. On the other hand, the capacity maintaining ratio of annealed sample below 400 °C was low: 18% after 30 cycles. To identify this reason, ESR measurement of annealed samples were carried out. In Fig. 7, ESR spectra of annealed samples at 200, 400 and 600 °C were shown. For the samples annealed at 400 °C, an evident micro wave absorption peaks were observed around the g value = 2.0 that were not found in samples annealed at other temperature. These peaks can be assigned to that of Mo(V) ion [30,31]. From this result, it was found that annealing of KPM at 400 °C under air causes the reduction of a slight part, not detectable by XRD, of Mo(VI) ion of KPM to Mo(V) and this reduction of molybdenum ion seems to cause fast capacity fading in the cycle performance. The ESR signal was not observed from the samples annealed above 500 °C. These results suggest a mechanism as follows. Annealing above 500 °C cause re-oxidization of Mo(V) to Mo(VI) and this oxidation would reorganize the crystal structure of KPM that was confirmed as new XRD reflections in Fig. 2(c). This re-organized surface by heat treatment above 500 °C seems to show higher cycle

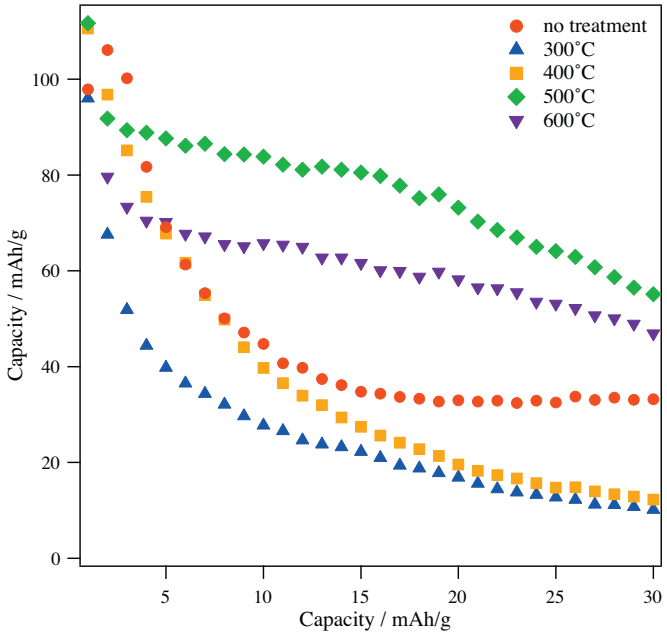

Fig. 6. Relationship between charge–discharge cycles and discharge capacity of $K_3[PMo_{12}O_{40}]$ annealed at various temperature.

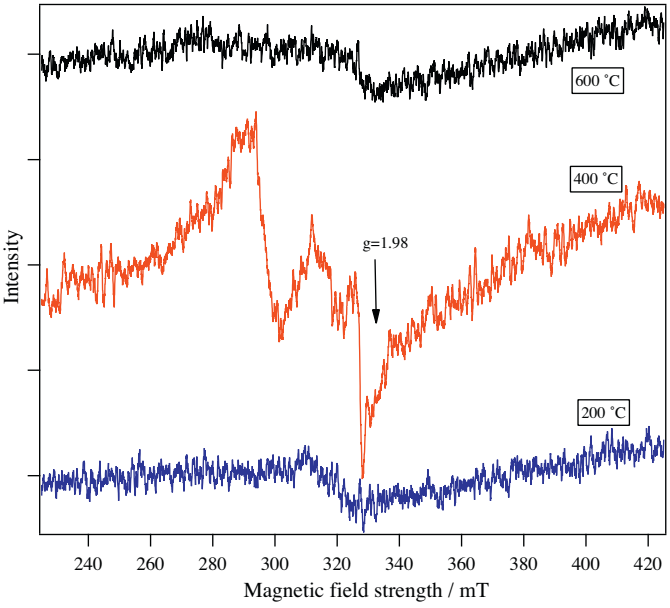

Fig. 7. ESR spectra for $K_3[PMo_{12}O_{40}]$ annealed at various temperature.

performance than the KPM without heat treatment. By annealing at 600 °C, the crystal structure seems to return to the original one.

The results in the present study demonstrated the possibility for KPM application to the cathode material with high capacity. For this application, a further stabilization of KPM crystal structure is necessary. The study for KPM structure stabilization is now under proceeding.

4. Conclusion

Lithium charge–discharge ability of KPM is demonstrated. This hetero polyoxomolybdate cluster ion showed possibility of new cluster ion type framework that can be developed for the lithium storage.

Acknowledgment

This work was financially supported by NEDO (New Energy and Industrial Technology Development Organization) Li-EAD project.

References

[1] H. Inside, K. Oyaizu, Science (Washington, DC, United States) 319 (5864) (2008) 737–738.
[2] S.A. Miller, C.R. Martin, Journal of the American Chemical Society 126 (20) (2004) 6226–6227.
[3] J.M. Cooper, R. Cubitt, R.M. Dalgliesh, N. Gadegaard, A. Glidle, A.R. Hillman, R.J. Mortimer, K.S. Ryder, E.L. Smith, Journal of the American Chemical Society 126 (47) (2004) 15362–15363.
[4] K. Oyaizu, Y. Ando, H. Konishi, H. Nishide, Journal of the American Chemical Society 130 (44) (2008) 14459–14461.
[5] J. Yamaki, A. Yamaji, Journal of the Electrochemical Society 129 (1) (1982) 5–9.
[6] S. Okada, J. Yamaki, T. Okada, Journal of the Electrochemical Society 136 (2) (1989) 340–344.
[7] N. Imanishi, T. Morikawa, J. Kondo, Y. Takeda, O. Yamamoto, N. Kinugasa, T. Yamagishi, Journal of Power Sources 79 (2) (1999) 215–219.
[8] N. Imanishi, T. Morikawa, J. Kondo, R. Yamane, Y. Takeda, O. Yamamoto, H. Sakaebe, M. Tabuchi, Journal of Power Sources 81–82 (1999) 530–534.
[9] H. Yoshikawa, C. Kazama, K. Awaga, M. Satoh, J. Wada, Chemical Communications (Cambridge, United Kingdom) (30) (2007) 3169–3170.
[10] F. Goubin, L. Guenee, P. Deniard, H.J. Koo, M.H. Whangbo, Y. Montardi, S. Jobic, Journal of Solid State Chemistry 177 (12) (2004) 4528–4534.
[11] G.A. Tsigdinos, Industrial and Engineering Chemistry Product Research and Development 13 (4) (1974) 267–274.
[12] T.V. Andrushkevich, V.M. Bondareva, G.Y. Popova, Y.D. Pankratiev, Reaction Kinetics and Catalysis Letters 52 (1) (1994) 73–80.
[13] G.Y. Popova, T.V. Andrushkevich, V.M. Bondareva, I.I. Zakharov, Kinetika i Kataliz 35 (1) (1994) 91–95.
[14] G.A. Tsigdinos, C.J. Hallada, Journal of the Less-Common Metals 36 (1/2) (1974) 79–93.
[15] E. Itabashi, Bulletin of the Chemical Society of Japan 60 (4) (1987) 1333–1336.
[16] K. Maeda, S. Himeno, T. Osakai, A. Saito, T. Hori, Journal of Electroanalytical Chemistry 364 (1–2) (1994) 149–154.
[17] K. Maeda, H. Katano, T. Osakai, S. Himeno, A. Saito, Journal of Electroanalytical Chemistry 389 (1–2) (1995) 167–173.
[18] P.J. Kulesza, L.R. Faulkner, J. Chen, W.G. Klemperer, Journal of the American Chemical Society 113 (1) (1991) 379–381.
[19] O. Nakamura, T. Kodama, I. Ogino, Y. Miyake, Chemistry Letters (1) (1979) 17–18.
[20] N. Kumagai, N. Kumagai, K. Tanno, Electrochimica Acta 32 (10) (1987) 1521–1526.
[21] F. Leroux, L.F. Nazar, Solid State Ionics 133 (12) (2000) 37–50.
[22] S. Komaba, N. Kumagai, R. Kumagai, N. Kumagai, H. Yashiro, Solid State Ionics 152–153 (2002) 319–326.
[23] Y. Jeannin, J.P. Launay, M.A.S. Sedjadi, Inorganic Chemistry 19 (10) (1980) 2933–2935.
[24] S. Himeno, T. Osakai, A. Saito, Bulletin of the Chemical Society of Japan 62 (4) (1989) 1335–1337.
[25] A. Aoshima, T. Yamaguchi, Nippon Kagaku Kaishi (12) (1985) 2237–2245.
[26] T. Tsai, M. Ai, A. Ozaki, Bulletin of the Chemical Society of Japan 54 (7) (1981) 2103–2106.
[27] N. Mizuno, T. Watanabe, M. Misono, Bulletin of the Chemical Society of Japan 64 (1) (1991) 243–247.
[28] Y. Konishi, K. Sakata, M. Misono, Y. Yoneda, Journal of Catalysis 77 (1) (1982) 169–179.
[29] M. Misono, Catalysis Reviews—Science and Engineering 29 (2–3) (1987) 269–321.
[30] H. Kon, N.E. Sharpless, Journal of Physical Chemistry 70 (1) (1966) 105–111.
[31] R.G. Hayes, Journal of Chemical Physics 44 (5) (1966) 2210–2212.